

# Light-in-flight recording. 5: Theory of slowing down the faster-than-light motion of the light shutter

Nils Abramson, Sven-Goran Pettersson, and Hakan Bergstrom

Light-in-flight recording by holography uses a picosecond pulse for the reference beam, which like a sheet of light intersects the hologram plate and produces a sensitivity area that with a speed faster than light moves over the plate like a light shutter. If, however, the front of the reference pulse by diffraction in a grating is tilted relative to its direction of motion, the velocity of the light shutter can be slowed down resulting in increased recording time. The practical result using a reflection grating was a true recording that corresponded to a time compression of two to one. To minimize distortions of the recorded pulse shape we studied intersections that are identical for apparent (ellipsoidal) and true (spheroidal) wavefronts.

## I. Introduction

Light-in-flight recording by holography<sup>1-3</sup> is based on the fact that an object beam is holographically recorded on a hologram plate only if this is simultaneously illuminated by a reference beam. If the latter consists of a picosecond pulse it will function like a picosecond shutter. Finally, let this reference pulse be in the form of a widened and collimated beam that illuminates the plate almost parallel to its surface. In that case a thin sheet of light, e.g., 1 ps thick (0.3 mm), intersects the plate along a line that, similar to a light shutter, moves over the plate with approximately the speed of light.

If the angle ( $\theta_i$  in Fig. 1) separating the reference beam from the normal to the plate is  $90^\circ$ , the velocity of the intersection will be exactly the speed of light. If  $\theta_i$  is smaller, the velocity will be larger than the speed of light. If finally  $\theta_i$  is zero, the velocity will be infinite, which simply means that the whole plate is simultaneously sensitive to object light. In a companion paper<sup>4</sup> the experimental aspects of this paper are presented.

## II. Reference Pulse

Let us take a closer look at Fig. 1. The collimated reference beam ( $R$ ) illuminates the hologram plate ( $H-H$ ) at the angle  $\theta_i$  to the normal. It consists of a pulse that has a temporal length of  $t$  and thus a spatial length of  $c \cdot t$ . Thus, a sheet of light is formed with a thickness of  $c \cdot t$ , that with the speed of  $c$  passes the plate. The intersection forms a line of sensitivity with thickness  $s$  which moves along the plate at a velocity faster than light. Mathematically it can be described as

$$v = \frac{c}{\sin\theta_i}, \quad (1)$$

$$s = \frac{c \cdot t}{\sin\theta_i}, \quad (2)$$

where  $v$  = the velocity of the sensitivity line (the light shutter),

$c$  = the speed of light,

$\theta_i$  = the angle between reference beam and plate normal,

$s$  = thickness of the sensitivity line (slit width), and

$t$  = temporal pulse length.

Thus, we have found that it is very easy to reach a velocity higher than that of light ( $\theta_i < 90^\circ$ ). However, a way to make the shutter velocity lower than that of light does not appear to exist, because  $\sin\theta_i$  cannot be larger than unity.

It is of course very satisfying to be able to produce a continuous, frameless 3-D film that records at a velocity higher than the speed of light, but sometimes a lower speed is advantageous because we want to study slower phenomena of longer duration.

Nils Abramson is with Royal Institute of Technology, Industrial Metrology, S-100 44 Stockholm, Sweden; the other authors are with Lund Institute of Technology, Physics Department, S-221 00 Lund, Sweden.

Received 15 March 1988.

0003-6935/89/040759-07\$02.00/0.

© 1989 Optical Society of America.

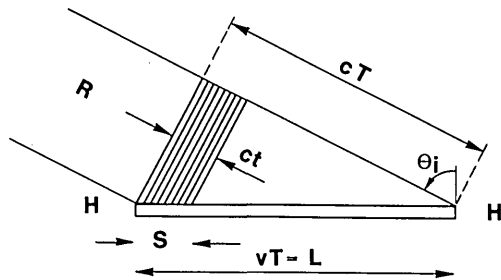


Fig. 1. Reference pulse ( $R$ ) with temporal length  $t$  illuminates the hologram plate ( $H-H$ ) at angle  $\theta_i$ . The pulse works like a light shutter with a slit width of  $S$  that during time  $T$  moves with velocity  $v$  along the plate of length  $L$ .

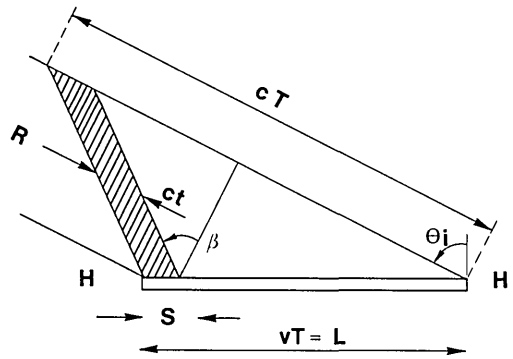


Fig. 2. Same as Fig. 1 but reference pulse ( $R$ ) is tilted angle  $\beta$  resulting in a lower velocity  $v$  and a longer recording time  $T$ .

### III. Increasing the Recorded Time Interval

The time span recorded by the hologram is

$$T = \frac{L \cdot \sin\theta_i}{c}, \quad (1)$$

where  $T$  = the resolved time interval,

$L$  = length of the hologram plate, and

$\theta_i$  = the angle of incidence for the reference beam.

If, for example, the hologram plate is 30 cm long and  $\theta_i$  is close to  $90^\circ$ , the time interval that can be recorded is limited to 1 ns. Many situations that we want to study with this method might be of longer duration, and the only possibilities to increase the time recorded appear to be as follows:

- (1) Increase angle  $\theta_i$  to  $90^\circ$ .
- (2) Increase the length of the hologram plate, e.g., by using a film instead of a plate.
- (3) Let the reference consist of several correlated beams that step by step have an increasing path length.
- (4) Decrease  $c$  by using a material of high refractive index.

However, one more possibility exists and that is to tilt the wavefront so that it is no longer normal to the travel of the light as seen in Fig. 2. The situation is identical to that of Fig. 1 but the wavefront is tilted at an angle  $\beta$  to the normal of the direction of the reference beam. When  $\beta$  is equal to zero the situation is identical to that of Fig. 1. If  $\theta_i$  is constant the velocity  $v$  will increase with decreasing  $\beta$  while an increasing  $\beta$  results in a decreasing  $v$ . The situation is described by the following equations:

$$v = \frac{c \cdot \cos\beta}{\sin(\theta_i + \beta)}, \quad (4)$$

$$s = \frac{c \cdot t \cdot \cos\beta}{\sin(\theta_i + \beta)}, \quad (5)$$

$$T = \frac{L \cdot \sin(\theta_i + \beta)}{c \cdot \cos\beta}, \quad (6)$$

where  $v$ ,  $c$ ,  $t$ ,  $T$ , and  $\theta_i$  represent the same quantities as in Eqs. (1)–(3).

However,  $\beta$  represents the angle between the wavefront and the normal to the motion of the reference beam as seen in Fig. 2. Equation (4) degenerates into

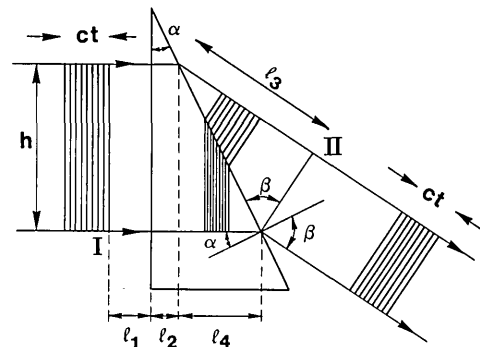


Fig. 3. Pulse with length  $ct$  is deflected by refraction in a prism at angles  $\beta - \alpha$ . After refraction the pulse front is still perpendicular to the direction of propagation and the pulse length is unchanged.

Eq. (3) if  $\beta$  is equal to zero. It also shows that  $\beta = -\theta_i$  results in  $v = \infty$ , while  $\beta = 90^\circ$  results in  $v = 0$ . To take another example,  $\theta_i = 30^\circ$  and  $\beta = 60^\circ$  result in  $v = 0.5c$ .

Thus we have found a simple way to vary the velocity of our light shutter from infinity to zero. Just one problem remains: The angle  $\beta$  is not allowed to differ from zero because by definition a wavefront is a line that is perpendicular to the direction of travel of the waves. To solve this problem we introduce the term pulse front instead of wavefront, to be used in all situations when the front is not perpendicular to the direction of travel.

### IV. Pulse Front Rotation

There are different ways to produce a pulse front that is inclined to the direction of travel. Let us first study why an ordinary prism does not rotate the pulse front (wavefront).

To study the deflection by refraction in a prism we choose the situation in Fig. 3 where light is bent downward. The lower part of the beam is delayed more than the upper part so that the wavefront is rotated just as much as the beam is deflected and therefore it is always perpendicular to the direction of travel. The delay is of course caused by the lower speed of light in the glass which is thicker at the lower part of the beam.

The separation of the two wavefronts is identical in space and time before and after the prism. Therefore

a pulse will not change its length and a sheet of light of a certain thickness will have that same thickness after the beam has been deflected downward.

Let us assume that a wavefront constitutes a surface that:

- (1) represents equal phase,
- (2) is perpendicular to the light rays,
- (3) represents equal time of flight, and
- (4) moves in such a way that every point on the front travels along a line of least (or most) time of flight (Fermat's principle).

The two first statements are true by definition, the third statement might at first glance appear to be a result of the others, while the fourth statement appears to be true by tradition.

For light not chopped up (e.g., light not diffracted) all the statements are true not only for wavefronts but also for pulse fronts. However, for diffracted light, statements (1) and (2) are true for wavefronts while statement (3) is the only one that is true for pulse fronts. (This shortcoming inspired a modification of Fermat's principle.<sup>5</sup>)

#### A. Comparison Between Prism and Grating

Let us first again study the refraction by a prism as described in Fig. 3. The optical path length from I to II for the top ray is  $L_T$  and for the bottom ray  $L_B$ :

$$L_T = n_0 l_1 + n_1 l_2 + n_0 l_3 = n_0 l_1 + n_1 l_2 + n_0 h \cdot \frac{\sin \beta}{\cos \alpha},$$

$$L_B = n_0 l_1 + n_1 l_2 + n_1 l_4 = n_0 l_1 + n_1 l_2 + n_1 h \cdot \tan \alpha,$$

where  $n_0$  is the refractive index of air and  $n_1$  is the refractive index of glass; all other notations are found in Fig. 3.

If our statements (2) and (3) are true,  $L_T$  should be equal to  $L_B$ . Thus  $L_T = L_B$  results in

$$n_0 \cdot \sin \beta = n_1 \cdot \sin \alpha.$$

In this way we have found that by assuming that our statements (2) and (3) are true we have arrived at Snell's formula of refraction which is a generally accepted formula. Statement (1) follows automatically from statement (3) and therefore all three statements appear to be true in the example studied.

The situation when light is deflected by diffraction in a grating is very different (see Fig. 4). No rays are delayed more than the others. The optical path length and thus the time of flight are solely determined by the path length itself. To make the situation simple and similar to that of Fig. 3 we let the incident light of Fig. 4 be normal to the surface of the grating. We see that the fronts of equal time (the pulse fronts) are all parallel to the original front independent of the diffraction angle. Thus the angle  $\delta$  that separates the diffracted beam from the zero-order beam is also the angle  $-\beta$  between the normal (to the travel of the light) and the pulse front. It is also seen that the thickness ( $l_1$ ) of the inclined sheet of light varies for light reflected in different directions.

Thus we have found that refraction by a prism does not tilt the wavefront or pulse front in relation to the

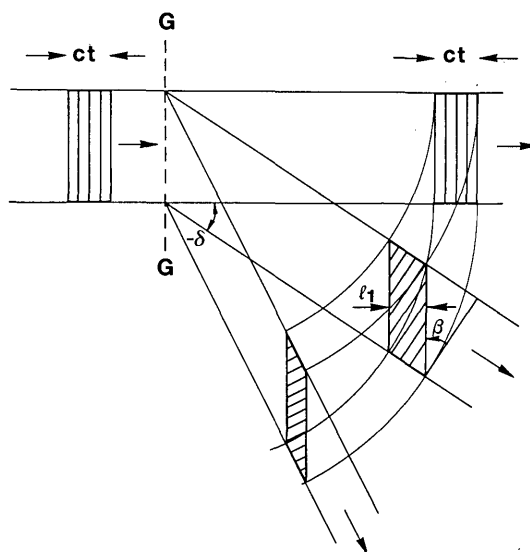


Fig. 4. Pulse with length  $ct$  is deflected by diffraction in a grating ( $G-G$ ) at angle  $\delta$ . The larger the angle  $\delta$  the thinner the light sheet  $l_1$ , while the length of the total pulse increases. The tilt of the pulse front is given by angle  $\beta = -\delta$ .

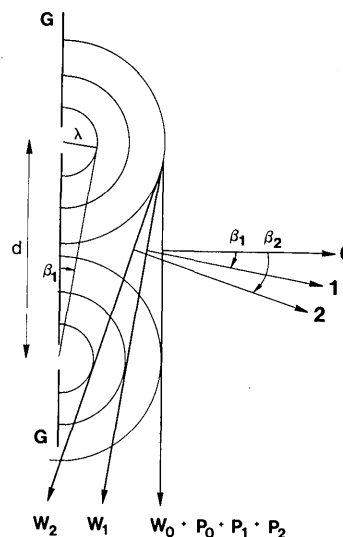


Fig. 5. Pulse arrives normal to grating ( $G-G$ ), which has a line separation of  $d$ . The beams of different orders leave at directions  $0$ ,  $\beta_1$ , and  $\beta_2$ , their wavefronts are  $W_0$ ,  $W_1$ , and  $W_2$ , respectively, but their pulse fronts  $P_0$ ,  $P_1$ , and  $P_2$  are all parallel to  $W_0$ .

direction of travel, neither does it change the temporal or spatial length of a pulse; the only change is in the diameter of the beam. A grating on the other hand tilts the pulse front, it also appears to change the temporal and spatial length of a pulse. To study the situation of Fig. 4 in more detail let us first look at Fig. 5.

We find that the angle  $\beta$  separating the angle of the pulse front from that of the normal to the light rays follows the equation

$$\sin \beta = \frac{n \cdot \lambda}{d}, \quad (7)$$

where  $n$  = diffracted order,  
 $\lambda$  = wavelength, and  
 $d$  = separation of the grating lines.  
 From Fig. 4 we also find

$$l_1 = c \cdot t \cdot \cos\beta, \quad (8)$$

where  $l_1$  = thickness of the light sheet after diffraction, and  
 $c \cdot t$  = thickness of the light sheet before diffraction.

### B. Grating, General Case

Until now we have studied the special situation when incident light is perpendicular to the grating. Let us now consider a more general case. First we evaluate graphically the distortion of a pulse diffracted by a reflection or transmission grating (see Fig. 6). A pulse front ( $P_0-P_0$ ) arrives at grating ( $G-G$ ) at angle  $\gamma$  and is diffracted in different directions at angle  $\delta$ .  $H$  is the point where the highest rays of the beam pass the grating, while  $L$  is the lowest point. The original incoming pulse front is assigned ( $P_0-P_0$ ), while the diffracted pulse front is ( $P_D-P_D$ ). By simply making the path lengths ( $P_0HP_D$ ) and ( $P_0LP_D$ ) equal for all the diffracted beams, we find the tilt angle  $\beta$  of all the pulse fronts including the retroreflected one. The pulse length along the light rays is identical for all beams, but the thickness of the light sheets varies. It is interesting to see that wavefronts and pulse fronts are identical and unchanged for the zero-order diffracted beams.

Now let us study the situation of Fig. 6 in more detail using trigonometry to calculate the path lengths (see Fig. 7). The difference in path length  $D$  between the highest and the lowest rays measured from ( $P_0-P_0$ ) to ( $P_D-P_D$ ) is

$$D = L_1 - L_2 = s \cdot (\sin\gamma - \sin\delta), \quad (9)$$

where  $s$  = separation along the grating between upper and lower studied rays,  
 $\gamma$  = angle of incidence for the incoming light beam, and  
 $\delta$  = angle of the diffracted light beam.

If we let  $s$  be the separation of the grating lines  $d$  and set the path length difference to an integer number  $n$  of wavelengths  $\lambda$  we get the usual equation for diffraction:

$$\sin\gamma - \sin\delta = \frac{n \cdot \lambda}{d}. \quad (10)$$

Now let us instead use Eq. (9) to evaluate the pulse front which is defined as the surface of zero path length difference for highest and lowest rays from the original pulse front (wavefront) to the diffracted pulse front ( $P_D-P_D$ ). The result is the following:

$$\tan\beta = \frac{\sin\gamma - \sin\delta}{\cos\delta}, \quad (11)$$

where  $\beta$  = angle between pulse front and normal to the diffracted light rays = the tilt angle and  $\gamma$  and  $\delta$  are the same notations as in Eq. (9). Thus with Eqs. (10) and (11) we have found the general formula for the tilt of

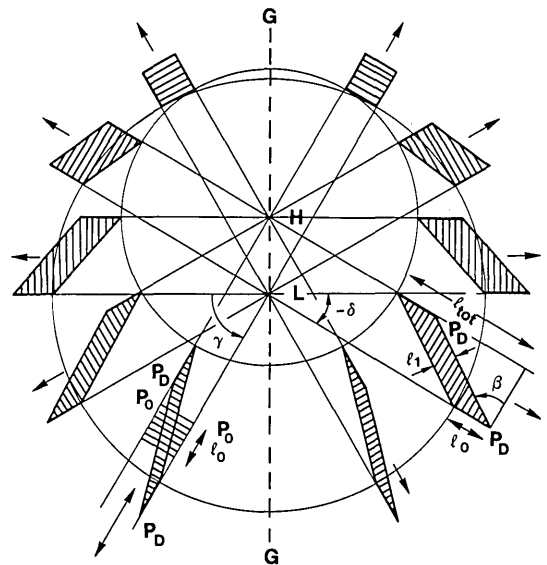


Fig. 6. General case of pulse front tilt. A pulse, as long as it is wide, moves toward grating ( $G-G$ ) at angle  $\gamma$ . By transmission and reflection it is deflected into several diffraction orders, of which we study the one in the  $\delta$  direction. All the angles are measured positive in the counterclockwise direction. For all diffraction orders, except the zero order, the pulse front is tilted at an angle  $\beta$ , the thickness of light sheet  $l_1$  is reduced, and the total pulse length  $l_{tot}$  is increased.

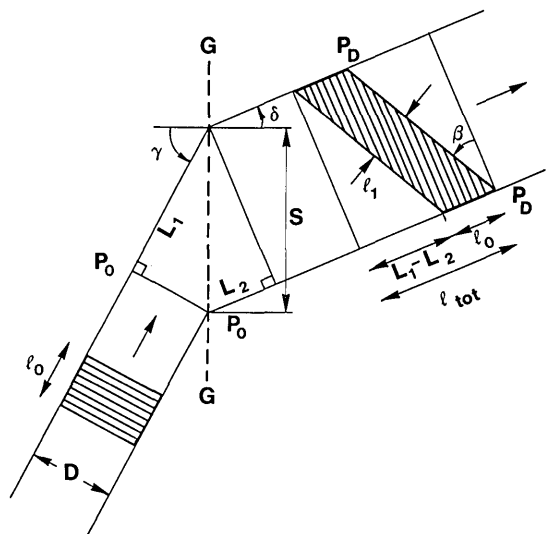


Fig. 7. Pulse front tilt angle  $\beta$  is calculated on the basis that the path lengths from the incoming wavefront ( $P_0-P_0$ ) to the outgoing pulse front ( $P_D-P_D$ ) are identical for the top ray ( $L_1$ ) and for the bottom ray ( $L_2$ ).

the pulse front caused by diffraction. If the incoming beam is perpendicular to the grating ( $\gamma = 0$ ), we get  $\beta = -\delta$  as stated in Eq. (7) and Figs. 4 and 5.

The tilt of the pulse front becomes zero for  $\delta = \gamma$  and for  $\delta = 180 - \gamma$  which both represent zero-order diffraction beams. Finally the tilt approaches a maximum of  $90^\circ$  for retroreflection ( $\delta = 180 + \gamma$ ) when  $\gamma$  approaches  $90^\circ$ . The thickness of light sheet  $l_1$  is

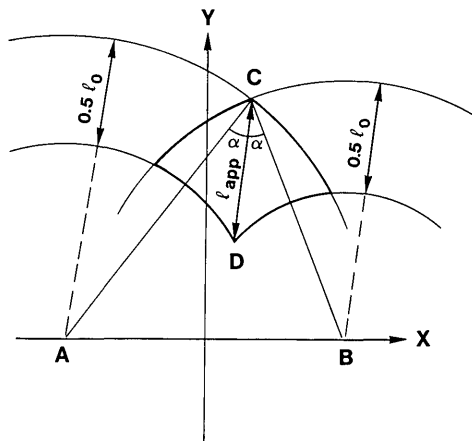


Fig. 8. Picosecond pulse with length  $l_0$  is emitted at A producing a spherical light sheet with thickness  $l_0$ . The pulse is scattered by smoke or small particles so that it can be observed at C using a picosecond observation from B. It then appears to be in the form of an ellipsoidal shell with thickness  $l_{app}$ , where  $l_{app} = k \cdot 0.5 l_0$ ,  $k = 1/\cos\alpha$ , and  $\alpha$  is half the angle ACB.

$$l_1 = l_0 \cdot \cos\beta, \quad (12)$$

where  $l_0$  is the length of the original pulse. The total temporal pulse length ( $t_{tot}$ ) as measured by a detector covering the whole beam diameter (see Fig. 7) is

$$t_{tot} = t_0 + \frac{D}{c} \cdot \frac{\sin\gamma - \sin\delta}{\cos\gamma}, \quad (13)$$

where  $D$  is the diameter of the incoming light. All the calculations made here have been based on simple trigonometry and do not take into account the diffraction-limited resolutions caused by the short pulses. As the pulse length of monochromatic light goes down, the light becomes less monochromatic due to the Fourier transform limit. Thus a very short pulse, say a few waves long, appears almost white, resulting in the diffraction-limited resolution having not only an ordinary spatial contribution, but also a temporal contribution. Another way to look at it is to say that the short pulse only illuminates a fraction of the grating simultaneously and therefore the shortness of the pulse has a temporal influence on the diffraction-limited resolution.

The equations given here agree well with our experiments made with pulses down to 12 ps ( $\sim 5 \times 10^3$  waves), while calculations show that corrections begin to be of importance when the pulses are  $< 100$  waves.

## VI. Object Beam

When a wavefront or pulse front is studied by light-in-flight (LIF) recording by holography or any other possible high-speed photography, the wavefront will appear distorted in time and space, because different points in space are recorded at different points in time because of the time delay caused by the limited speed of light used for observation.

Thus a flat wavefront that passes by appears tilted at  $45^\circ$ . A closer look reveals that a flat wavefront not only appears tilted but also transformed into a paraboloid, its focal point being the point of observation (e.g.,

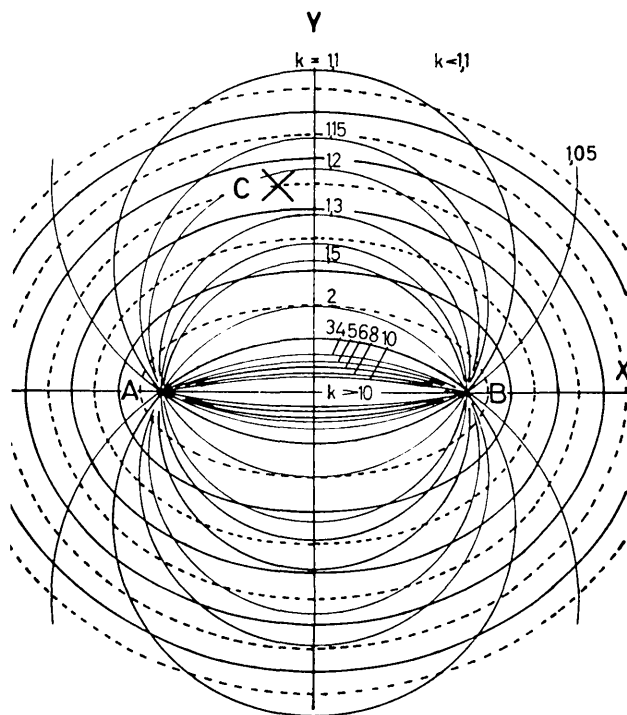


Fig. 9. Holodiagram originally designed for the evaluation of holographic interference fringes. The apparent pulse length is represented by the separation of the ellipses with a constant  $k$  value along arcs of circles. This  $k$  value ( $k = l_{app}/0.5 l_0$ ) is equal to unity along the  $x$  axis to the right of observation point B and to the left of the point for illumination A. Everywhere else the  $k$  value is higher and between A and B it is infinite.

the studied point of the hologram plate). A spherical wavefront emitted from point A appears transformed into one of the ellipsoids of the holodiagram where A is one focal point and the point of observation B is the other. If A is at infinite distance from B the ellipsoids are transformed into the already mentioned paraboloids (see Fig. 9).

### A. Ellipsoids of the Holodiagram

The apparent length of the pulse is equal to the separation of the two ellipsoidal shells that represent the front and the end of the pulse. The relation between the apparent pulse length to the true pulse length is

$$l_{app} = k \cdot 0.5 \cdot l_{true},$$

where  $l_{app}$  = apparent spatial pulse length,  
 $l_{true}$  = true spatial pulse length =  $c \cdot t_0$ ,  
 $t_0$  = original temporal pulse length,  
 $k$  = the  $k$  value of the conventional holodiagram =  $1/\cos\alpha$ , and  
 $\alpha$  = half the angle separating illumination and observation directions (see Fig. 8).

The spheres appear ellipsoidal because light transmitted from A to B via the ellipsoidal surface represents a constant path length and thus constant time delay between emittance and detection of the pulse. The factor 0.5 is caused by the fact that light goes to the

ellipsoidal surface and back again. It is exactly the same phenomena as in interferometry but the wavelength is substituted by the pulse length.

The true 3-D shape of a wavefront (pulse front) can be seen only in the case when the separation of *A* and *B* is zero. In all other situations the ellipsoids differ from the spheres (see Fig. 9). Very often a sideways look at the wavefront is preferred and then a certain distance between *A* and *B* is needed; in that case it would also be useful to have an undistorted view. Even if the apparent 3-D shape of the wavefront differs from its true shape it is, however, still possible to find cross sections of the ellipsoids with focal points *A* and *B* that are identical to cross sections of spheres centered at *A*. These cross sections reveal the true spatial and temporal shapes of any pulse or wavefront.

### B. Undistorted Wavefront

To find this undistorted wavefront we should study the intersection produced by a screen that is as parallel to the light rays as possible. To see the total intersection at the same point of time the screen should be perpendicular to the direction of observation *B*. From Fig. 10, which visualizes the ellipsoids as caused by the moire effect of spheres, we see that along a circle centered at *B* the intersections by the ellipsoids are identical to the intersections by circles centered at *A*. Thus, if a spherical screen with its center at *B* is illuminated by light from *A* the intersections by the ellipsoids are identical to those by the spherical wavefronts emitted by *A*. We choose this configuration but for simplicity we accept the approximation made by using a flat surface at a large distance from *B* instead of a spherical one. In this way we also become more or less independent of the position of *A* as long as it is close to the surface of the screen. The result is that we should position a flat screen so that its surface almost intersects the point of illumination *A* while its normal intersects the point of observation *B* at a large distance.

Now let us finally see how the proposed setup agrees with results from the hodiogram of Fig. 9. The angle of 90° between illumination and observation directions corresponds to a *k* value of  $1/\cos 45^\circ = \sqrt{2}$ . Thus the pulse length  $c \cdot t_0$  results in a separation of  $0.5 \cdot \sqrt{2} \cdot c \cdot t$  between the ellipsoids representing the front and the end of the pulse (apparent 3-D pulse length). For the *k* values of  $\sqrt{2}$  studied, which is situated on a circle through *A* and *B*, the screen is everywhere at an angle of almost 45° to the ellipsoids. Thus the pulse length as seen on the screen is identical to the true pulse length ( $0.5 \cdot \sqrt{2} \cdot \sqrt{2} \cdot ct = ct_0$ ).

## VII. Conclusion

This work has been made to demonstrate in a general way that the behavior of short pulses is in many respects different from that of continuous light. Thus both pulse shape and pulse length are changed after a pulse is diffracted by a grating. Equations have been given to explain these changes. It is, for example, important to note that the pulse length of a tilted pulse appears different when measured holographically

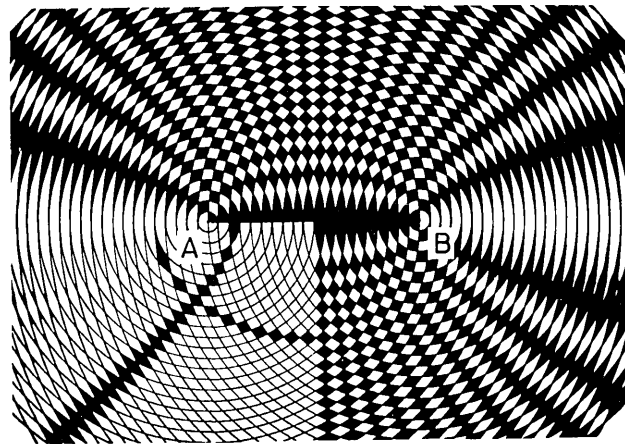


Fig. 10. Another way to visualize the hodiogram in Fig. 9. *A* and *B* are the centers of sets of concentric circles in a bipolar coordinate system. The moire fringes form a set of ellipses. To emphasize this pattern every second rhomboid area is painted black except for one-quarter of the diagram where just one single ellipse (and hyperbola) has been marked. The ellipses are formed where circles around *A* intersect circles around *B*. Therefore, a spherical screen centered at *B* will be intersected by spherical wavefronts from *A* in exactly the same way as it will be intersected by the ellipsoids. Thus projected on this screen the apparent pulse shape and pulse length will be identical to those of the true pulse.

compared to the total pulse time measured using a photoelectric detector. This means that, when a short pulse is used in combination with a grating, in, e.g., a monochromator, the pulse length as seen by a detector is increased and this fact must be taken into account when doing time-resolved measurements. We also show how an experimental setup should be designed to make a true image of pulse fronts recorded in a light-in-flight experiment. A tilted pulse front was used to expand the view time of a light-in-flight recording. The theoretical result was verified by a successful experiment where the recording time was doubled, as described in a companion paper.<sup>4</sup>

The development of light-in-flight recording by holography has been sponsored by the Swedish Board for Technical Development whose interest and support are gratefully acknowledged.

## Appendix

The pulse front concept is also useful in understanding white light interferometry. A conventional interferometer is seen in Fig. 11. Light of short pulse length or short temporal coherence length (*P*) arrives from the lower left and is divided by a beam splitter (*BS*) into two symmetrical beams that are combined at *C* by two mirrors (*M*). Because the pulse fronts are always perpendicular to the beam directions, fringes are formed only inside the rhomb at *C* where the two pulses intersect. The rhomb moves from left to right and the number of fringes within the height of the rhomb is calculated:

$$n = \frac{H}{d},$$

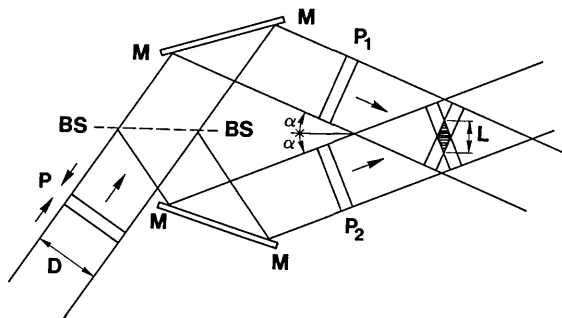


Fig. 11. Conventional interferometer is illuminated by a light beam of short pulse length or short temporal coherence length that arrives from the lower left. It is divided by the beam splitter (BS) into two symmetrical beams that combine at C after reflection in two mirrors. The angle  $2\alpha$  separating the two intersecting pulse fronts restricts the number of fringes produced only within the rhomb with height  $H$ .

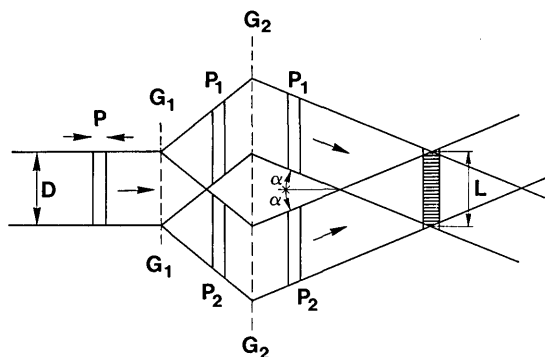


Fig. 12. Corresponding grating interferometer with the same illumination as in Fig. 11. Grating  $G_1$  divides the beam while another grating  $G_2$  recombines the two beams. As the two intersecting pulse fronts are parallel, they cover each other totally and interference fringes are produced across the whole area of the beam. Thus even white light produces a large number of fringes.

$$H = \frac{P}{\sin\alpha}, \quad (\text{A1})$$

$$d = \frac{\lambda}{2 \sin\alpha}.$$

Thus

$$n = \frac{2P}{\lambda},$$

where  $n$  = number of fringes formed,  
 $H$  = height of rhomb,  
 $d$  = fringe separation,  
 $P$  = the pulse length or temporal coherence length,  
 $\alpha$  = half of the angle separating the intersection beams, and  
 $\lambda$  = the wavelength.

The result shows that for  $H < D$  the number of fringes formed is simply twice the number of waves within the pulse length or the temporal coherence length.

As a contrast in Fig. 12 we show a grating interferometer that functions with a white light source.<sup>6</sup> Light of short pulse length arrives from the left and is divided by grating  $G_1$  into two symmetrical beams combined at C by grating  $G_2$ . Because the pulse fronts are always parallel to the original pulse front (vertical), the two pulses cover each other completely. Therefore fringes are formed across the whole beam area. Thus

$$n = \frac{2D \sin\alpha}{\lambda}.$$

This result shows that the number of fringes for the grating interferometer is not limited by pulse length or coherence length.

#### References

1. N. Abramson, "Light-in-Flight Recording by Holography," *Opt. Lett.* **3**, 121 (1978).
2. N. Abramson, "Light-in-Flight Recording: High-Speed Holographic Motion Pictures of Ultrafast Phenomena," *Appl. Opt.* **22**, 215 (1983).
3. N. Abramson, "Light-in-Flight Recording. 2: Compensation for the Limited Speed of the Light Used for Observation," *Appl. Opt.* **23**, 1481 (1984).
4. S. Petterson, H. Bergstrom, and N. Abramson, "Light-in-Flight Recording. 6: Experiment with View-Time Expansion Using a Skew Reference Wave," *Appl. Opt.* **28**, xxxx (1989).
5. N. Abramson, "Principle of Least Wave Change," *J. Opt. Soc. Am. A or B*, submitted.
6. E. N. Leith and B. J. Chang, "Image Formation with an Achromatic Interferometer," *Opt. Commun.* **23**, 217 (1977).